CrystEngComm

Accepted Manuscript

ROYAL SOCIETY OF CHEMISTRY

www.rsc.org/crystengcomm

Use of the oxime-oximato binding mode to stabilise mixed valence copper iodide polymer networks using dipyridyl ketone oxime ligands.

Victoria J. Argyle, Marina Roxburgh and Lyall R. Hanton *

Received (in XXX, XXX) Xth XXXXXXXXX 20XX, Accepted Xth XXXXXXXXX 20XX
DOI: 10.1039/b000000x

Five complexes prepared from CuI and dipyridyl ketone oxime ligands were synthesised and structurally characterised, $[Cu_2I_2(\mathbf{L^{23}})(\mathbf{L^{23}}\text{-H})]_\infty$, **1**, $[Cu(\mathbf{L^{23}}\text{-H})_2]_\infty$, **2**, $\{[Cu_2(\mathbf{L^{24}})(\mathbf{L^{24}}\text{-H})I_2](CH_3CN)\}_\infty$, **3**, $[Cu(\mathbf{L^{33}})I]_\infty$, **4**, and $\{[Cu_8(\mathbf{L^{44}})_5I_8](CH_3CN)_4(C_4H_{10}O)_2(H_2O)_2\}_\infty$, **5**. The effect of the varying pyridyl substitution patterns of $\mathbf{L^{23}}$, $\mathbf{L^{24}}$, $\mathbf{L^{33}}$ and $\mathbf{L^{44}}$ was investigated, as well as the effect this had on forming mixed valence complexes. Complexes **1** and **3** formed mixed valence Cu(I)/Cu(II) polymer networks with Cu(II) stabilised by the formation of a pseudo tetradentate ligand through an oxime-oximato bridge. In comparison, the Cu(I) in complex **2** was completely oxidised to Cu(II), with the ligand fully deprotonating to act as a charge balance. Complex **4** formed a simple 1D Cu_2I_2 rhomboid dimer daisy chain, while **5** formed Cu_4I_4 cubane tetramer clusters, allowing four ligands to bind to one centre. Overall **5** existed as two interpenetrated hydrogen bonded 3D networks. Introduction

Complexes of copper iodide form very diverse structures for a number of reasons. Cu(I) can have coordination numbers typically ranging from two to four, and Cu(II) from four to six. Iodide can form terminal, or μ-bridging arrangements allowing a wide range of binding modes.[1] Commonly, Cu(I) iodide aggregates as rhomboid dimers, cubane tetramers and stepped cubane tetramers, allowing the expansion of these clusters into coordination polymers due to vacant metal coordination sites which provide useful scaffolding for coordination polymer networks.[1, 2] In comparison, Cu(II) iodide structures are rare,[3] and dominated by Jahn-Teller elongated Cu-I bonds, which often bridge to form coordination polymers[4].

Given the wide range of structures available for copper iodide complexes, we prepared coordination polymer architectures using the versatile four isomeric ligands, 2,3-, 2,4-, 3,3′- and 4,4’-dipyridyl ketone oxime ($\mathbf{L^{23}}$, $\mathbf{L^{24}}$, $\mathbf{L^{33}}$ and $\mathbf{L^{44}}$ respectively) (Fig. 1). In engineering these coordination polymers, such ligands offer a number of advantages when combined with copper iodide. Both the oxime functional group and the pyridyl donors have the ability to bind to metal ions, and to form H-bonding interactions. This allows the complexes to extend further into coordination polymers, and examples of these binding modes were observed in **1-5**. Rotation around the C_{py}–C_{ox} (py = pyridine; ox= oxime) bond allows a degree of freedom, however in the cases of $\mathbf{L^{23}}$ and $\mathbf{L^{24}}$ this can be hindered by the formation of a five-membered chelate ring between the 2-substituted ring and the N atom of the oxime unit.

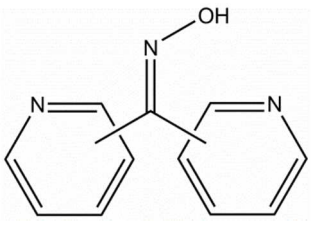

Fig. 1 Schematic representing the four isomeric dipyridyl ketone oxime ligands $\mathbf{L^{23}}$, $\mathbf{L^{24}}$ $\mathbf{L^{33}}$ and $\mathbf{L^{44}}$.

When solvated, Cu(I) iodide is susceptible to oxidation to Cu(II) in air. Any corresponding reduction of Cu(II) to Cu(I) by iodide is inhibited by the presence of a N_{py} donor resulting in the formation of Cu(II)–N_{py} bound complexes with coordinated iodide.[4,5] In previous copper complexes with 2,2’-dipyridyl ketone oxime the five-membered-chelate ring can be further extended into a pseudo tetradentate ligand through the presence of an oxime-oximato bridge in neighbouring ligands (fig. 2).[6] Often in this oxime-oximato bridge the hydrogen is thought to be shared almost equally between the two oxygen atoms. This motif is valuable in crystal engineering, and provides a very strong coordination motif for Cu(II).[7] The deprotonation of oximes is often observed, and allows the ligand to act as a counter ion helping to balance the charge formed by oxidation. The oxidation of Cu(I) to Cu(II) is not uncommon in solvothermal reactions, however mixed valance Cu(I)/Cu(II) coordination polymers are still relatively rare. It would follow that the formation of a mixed valence polymer from room temperature solvent diffusion is even more unusual, which was observed in **1** and **3**.

Interestingly, structures containing Cu(II) bound in a pseudo tetradentate fashion through an oxime-oximato bridge between neighbouring ligands were some of the first oxime structures, reported in 1961.[8] Previous summaries identify the oxime-

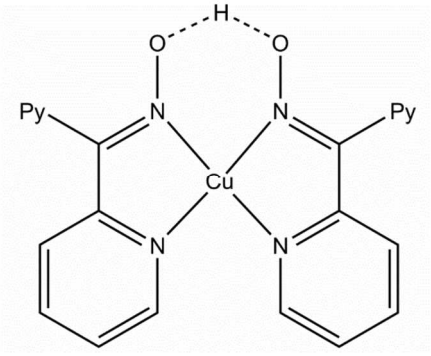

Fig. 2 Diagram of the pseudo tetradentate ligand formed by an oxime-oximato bond on complexation with copper.

oximato bridge as quite common,[9] however the ability of an oxime ligand to bind further by forming five-membered chelating ring, using an ancillary donor group such as pyridine, is less well documented (Fig. 2). This pseudo tetradentate oxime-oximato bridge arrangement appears to have been overlooked[10-12] rather than being identified as a strong motif facilitating the binding, and strengthening the coordination of Cu(II).

Herein are reported five CuI complexes (**1**-**5**) of four regio isomer ligand entities, $\mathbf{L^{23}}$, $\mathbf{L^{24}}$, $\mathbf{L^{33}}$ and $\mathbf{L^{44}}$, respectively (Fig. 1). Of these, two were mixed-valence complexes, prepared by the spontaneous oxidation of Cu(I) ions. X-ray structural analysis was used to investigate the effect the N_{py} position had on the nature of the polymer network, and how the different oxidation states were stabilized. Complex **1** formed a mixed valence Cu(I)/Cu(II) 2D polymer with Cu(II) stabilised by the formation of a pseudo tetradentate ligand through an oxime-oximato bridge, and I- acting as a bridge between the Cu of the same oxidation states. In **2** all of the Cu(I) was oxidised to Cu(II), causing the ligand to fully deprotonate and act as the counter ion. Complex **3** was also mixed valence stabilised by the same binding motif as **1**, however the I- acted as a linker between Cu ions of differing oxidation states, forming an infinite 1D double chain. Complex **4** could no longer form a five-membered chelate ring to potentially stabilise Cu(II), so oxidation was not favoured, causing a simple 1D Cu_2I_2 rhomboid dimer daisy chain to form. Complex **5** formed Cu_4I_4 cubane tetramer clusters, allowing four ligands to bind to one centre, and existed overall as two interpenetrated hydrogen bonded 3D networks.

Experimental Section

General.

All chemicals were used as received without further purification. The ligands $\mathbf{L^{23}}$, $\mathbf{L^{24}}$, $\mathbf{L^{33}}$ and $\mathbf{L^{44}}$ were prepared according to literature methods[13]. All solvents were used as received, and were of LR grade or better. Elemental microanalyses were carried out at the Campbell Microanalytical Laboratory, University of Otago. Electrospray mass spectrometry was recorded on a Bruker micrOTOF-Q spectrometer in MeOH solutions. Data are presented as *m/z* values for the parent molecular ion. Infrared (IR) spectra were measured with either a Perkin Elmer Spectrum BX FT-IR System using KBr disks or a Bruker Optics Alpha FT-IR spectrometer (with a diamond Attenuated Total Reflectance (ATR) top-plate). Solid-state electronic spectra were collected as a $BaSO_4$ diluted sample with a Cary 500 UV-Vis-NIR spectrophotometer fitted with a 110 mm PTFE coated integrating sphere.

Syntheses.

$[Cu_2I_2(L^{23})(L^{23}\text{-}H)]_\infty$, 1, and $[Cu(L^{23}\text{-}H)_2]_\infty$, 2.

CuI (25 mg, 0.13 mmol) dissolved in CH_3CN (10 mL) was added to $\mathbf{L^{23}}$ (52 mg, 0.26 mmol) dissolved in CH_3OH (10 mL). The dark red solution was stirred overnight during which time a precipitate formed and the solution changed colour to olive green. The solid was filtered, washed with diethyl ether and dried *in vacuo* (38 mg, 38%). Two different types of dichroic X-ray quality crystals were obtained, which were green/red (**1**) and green/orange (**2**) in colour. They were grown together from the slow diffusion of a CH_3OH solution of $\mathbf{L^{23}}$ (20 mg, 0.10 mmol) layered with CH_3CN into a CH_3CN solution of CuI (19 mg, 0.10 mmol) layered with CH_3CN. The bulk material above was found to be consistent with the structure obtained from the red crystals (**1**). Anal. Found: C, 33.88; H, 2.23; N, 10.65. Calc. for $C_{22}H_{17}N_6O_2Cu_2I_2$: C, 33.95; H, 2.20; N, 10.80. EMS (+ve ESI) *m/z* calc for $C_{22}H_{18}N_6O_2Cu$ 461 $[(\mathbf{L^{23}})_2Cu(I)]^+$, found 461. Calc for $C_{22}H_{17}N_6O_2Cu$ 460 $[(\mathbf{L^{23}})(\mathbf{L^{23}}\text{-}H)Cu(II)]^+$, found 460. Selected IR (KBr)/cm^{-1}: 3446 (*s*, br) ($\mathbf{L^{23}}$), 3091-2923 (*w*, sh) ($\mathbf{L^{23}}$), 1597 (*m*, sh) ($\mathbf{L^{23}}$), 1540-1466 (*s*, sh) ($\mathbf{L^{23}}$), 998 (*w*, sh) ($\mathbf{L^{23}}$), 979 (*w*, sh) ($\mathbf{L^{23}}$), 800-780 (*m*, sh) ($\mathbf{L^{23}}$). UV-Vis ($BaSO_4$) (relative absorption)/ cm^{-1}: 41 667 (1), 27 948 (0.87), 22 344 (0.70), 16 436 (0.26), 11 614 (0.19), 5978 (0.42).

$\{[Cu_2(L^{24})(L^{24}\text{-}H)I_2](CH_3CN)\}_\infty$, 3.

CuI (49 mg, 0.26 mmol) dissolved in CH_3CN (10 mL) was added to $\mathbf{L^{24}}$ (52 mg, 0.26 mmol) dissolved in CH_3OH (10 mL). A red-brown precipitate immediately formed. The red solution was stirred overnight during which time the precipitate changed colour to dark brown. The solid was filtered, washed with diethyl ether and dried *in vacuo* (85 mg, 42%). Black X-ray quality crystals of **3** were grown from the slow diffusion of a CH_3OH solution of $\mathbf{L^{24}}$ (20 mg, 0.10 mmol) layered with CH_3OH into a CH_3CN solution of CuI (20 mg, 0.10 mmol) layered with CH_3CN. Anal. Found: C, 34.00; H, 2.47; N, 10.94. Calc. for $C_{22}H_{17}N_6O_2Cu_2I_2$: C, 33.95; H, 2.20; N, 10.80. Selected IR (KBr)/cm^{-1}: 3446 (*s*, br) ($\mathbf{L^{24}}$), 3053 (*w*, sh) ($\mathbf{L^{24}}$), 1653 (*w*, sh) ($\mathbf{L^{24}}$), 1595 (*m*, sh) ($\mathbf{L^{24}}$), 1542 (*w*, sh) ($\mathbf{L^{24}}$), 1466 (*m*, sh) ($\mathbf{L^{24}}$), 986 (*w*, sh) ($\mathbf{L^{24}}$), 826 (*m*, sh) ($\mathbf{L^{24}}$), 789 (*s*, sh) ($\mathbf{L^{24}}$), 746 (*m*, sh) (L^{24}). UV-Vis ($BaSO_4$) (relative absorption)/ cm^{-1}: 31 746 (1), 11 223 (0.32).

$[Cu(L^{33})I]_\infty$, 4.

CuI (49 mg, 0.26 mmol) dissolved in CH_3CN (10 mL) was added to $\mathbf{L^{33}}$ (52 mg, 0.26 mmol) dissolved in CH_3OH (10 mL). A white suspension resulted. This was stirred overnight during which time a cream precipitate formed. This was filtered, washed with diethyl ether and dried *in vacuo* (63 mg, 62%). Yellow X-ray quality crystals of **4** were grown from the slow diffusion of a CH_3OH solution of $\mathbf{L^{33}}$ (20 mg, 0.10 mmol) layered with CH_3CN into a CH_3CN solution of CuI (19 mg, 0.10 mmol) layered with CH_3CN. Anal. Found: C, 33.88; H, 2.38; N, 10.66. Calc. for $C_{11}H_9N_3OCuI$: C, 33.91; H, 2.33; N, 10.78. Selected IR (KBr)/cm^{-1}: 3256 (*s*, br) ($\mathbf{L^{33}}$), 3045-2809 (*w*, sh) ($\mathbf{L^{33}}$), 1638-1619 (*w*, sh) ($\mathbf{L^{33}}$), 1591 (*w*, sh) ($\mathbf{L^{33}}$), 1474 (*w*, sh) ($\mathbf{L^{33}}$), 1337 (*w*, sh) ($\mathbf{L^{33}}$), 960 (*w*, sh) ($\mathbf{L^{33}}$), 944 (*m*, sh) ($\mathbf{L^{33}}$), 931 (*m*, sh) ($\mathbf{L^{33}}$), 818 (*m*, sh) ($\mathbf{L^{33}}$).

$\{[Cu_8(L^{44})_5I_8](CH_3CN)_4(C_4H_{10}O)_2(H_2O)_2\}_\infty$, 5

CuI (50 mg, 0.26 mmol) dissolved in CH_3CN (10 mL) was added to $\mathbf{L^{44}}$ (52 mg, 0.26 mmol) dissolved in CH_3OH (10 mL). The resulting yellow solution was concentrated, and added to excess diethyl ether to give a white suspension. This was stirred overnight to give a yellow precipitate which was filtered, washed with diethyl ether and left to dry (45 mg, 55%, based on $\mathbf{L^{44}}$). Anal. Found: C, 29.55; H, 2.23; N, 8.66. Calc. for $C_{55}H_{45}N_{15}O_4Cu_8I_8{\cdot}2CH_3CN{\cdot}2C_4H_{10}O$: C, 29.26; H, 2.60; N, 8.66. Selected IR (ATR)/cm^{-1}: 1597 (w, sh) ($\mathbf{L^{44}}$), 1415 (m, sh) ($\mathbf{L^{44}}$), 1009 (s, sh) ($\mathbf{L^{44}}$). The slow diffusion of a CH_3OH solution of

L[44] (18.3 mg, 0.092 mmol) into a CH_3CN solution of CuI (16.3 mg, 0.086 mmol) layered with CH_3CN gave a yellow solution after 5 days. This was diffused with diethyl ether to give yellow coloured X-ray quality crystals.

X–Ray Crystallography.

X-Ray diffraction data were collected at the University of Otago on a Bruker APEX II CCD diffractometer, with graphite monochromated Mo-Kα (λ = 0.71073 Å) radiation. Intensities were corrected for Lorentz and polarisation effects[14, 15] and a multiscan absorption correction[16] was applied to all structures. The structures were solved by direct methods using SIR-97[17] and refined on F^2 using all data by full-matrix least-squares procedures (SHELXL 97[18]). Non-hydrogen atoms were refined with anisotropic thermal parameters. H atoms were placed in ideal positions except for the H atoms of the hydrido-bridged oxime-oximato units in **1** and **3**, and the oxime of **4**, which were located from the Fourier synthesis maps. All calculations were performed using the WinGX interface.[19] Detailed analyses of the extended structure were carried out using PLATON[97] and MERCURY[20, 21] (Version 1.4.2). Crystal data and refinement details are summarised in Table 1.

Results and Discussion

The isomeric dipyridyl oxime ligands were synthesised by literature methods.[13] All reactions were attempted in bulk with a 1:1 metal to ligand ratio. With the exception of **2** and **5** molar ratios of the isolated compounds were consistent with the initial stoichiometric ratios. In **2** the oxime unit was fully deprotonated giving rise to Cu(II) centres by auto oxidation. By comparison, the oxime unit in **1** and **3** formed a bridged oxime-oximato pseudo-tetradentate ligand stabilising the Cu(II) centre and giving rise to mixed valence Cu(I) and Cu(II) centres. All complexes were isolated as insoluble coordination polymers.

$[Cu_2I_2(L^{23})(L^{23}\text{-}H)]_\infty$, 1, and $[Cu(L^{23}\text{-}H)_2]_\infty$, 2

Dichroic green/red and green/orange X-ray quality crystals were grown from the slow diffusion of a MeOH solution of L^{23} into a MeCN solution of CuI. The green/red crystals, **1,** were found to have a 1:1 ligand-to-metal ratio and the green/orange crystals, **2,** had a 1:2 ligand-to-metal ratio. Both types of crystals had similar morphologies. Bulk reactions with varying molar ratios of L^{23} and CuI were carried out many times in a 1:1 mix of MeCN and MeOH giving dark red solutions initially. The 1:1 bulk reactions yielded materials which gave variable and inconsistent microanalyses. In contrast, the 2:1 bulk reactions gave only **1** as a dark green solid. Notably, the red solutions changed over time to olive green and dark green solid precipitated out. The bulk reactions never yielded material with microanalyses consistent with **2**.

Electrospray mass spectrometry of both the dark red and olive green solutions was carried out under normal operating conditions. The spectra showed a subtle change as the sample aged. The red solution showed a peak at 461 *m/z* which was assigned as $[(L^{23})_2Cu(I)]^+$. The olive green solution showed a peak at 460 *m/z* which was assigned as $[(L^{23})(L^{23}\text{-}H)Cu(II)]^+$. Thus, over time it appeared that the Cu(I) ion was being oxidized (Fig. 3).

IR analysis of the **1** showed peaks at 3446, 1597, 1540-1466 and 979 cm^{-1} which were consistent with L^{23}. The notable shift of the peak corresponding to the stretch of the C=N moiety from 1636 cm^{-1} as observed for the free ligand to 1597 cm^{-1} provided confirmation that L^{23} was coordinated to a Cu ion through the C=N moiety. The electronic spectrum of **1** showed a broad and intense charge transfer peak at 22 344 cm^{-1}, with a shoulder at 16436 cm^{-1}. A broad and asymmetric peak corresponding to the *d-d* transition of the metal ion was observed at 11 614 cm^{-1} confirming the presence of Cu(II). Such a spectral pattern would be consistent with the Cu(II) ion adopting either a square-pyramidal or Jahn-Teller distorted octahedral geometry.[22] The crystal structure of **1** showed that the Cu(II) ion had adopted a distorted octahedral geometry.

X-Ray structural analysis of **1** revealed the formation of a mixed-valence Cu(I) and Cu(II) complex, forming an infinite 2D network lying in the plane (1 0 -1). The network crystallized in the monoclinic space group $P2_1/n$ with the asymmetric unit containing one Cu(I) ion, one Cu(II) ion, two L^{23} ligands of which one was deprotonated, and two I^- anions. Given the centrosymmetric nature of the space group, both enantiomeric forms of L^{23} were found to be present in the crystal structure, however only one form of L^{23} was bound to each Cu(II) ion.

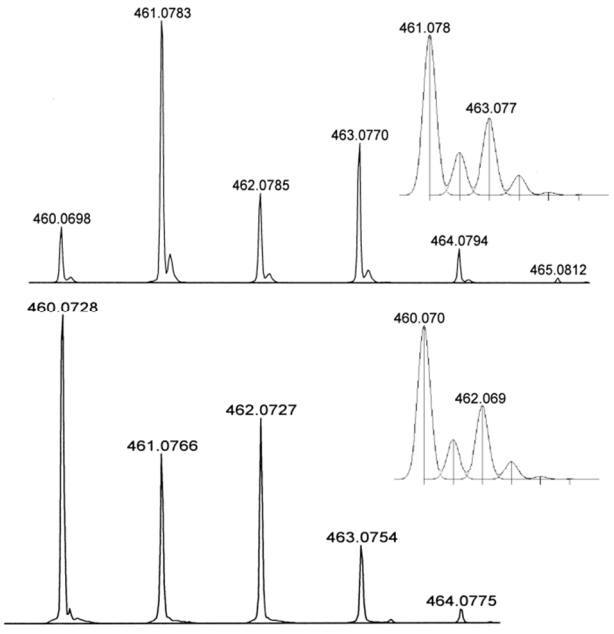

Fig. 3 (top) Positive ion electrospray mass spectrum showing the isotope pattern of the freshly prepared red solution in MeOH, showing the peak at *m/z* assigned to $[(L^{23})_2Cu(I)]^+$. (bottom) Isotope pattern of the aged olive green solution in MeOH showing the peak at *m/z* assigned to $[(L^{23})(L^{23}\text{-}H)Cu(II)]^+$. Insets show calculated isotope pattern for each of the copper species.

	1	2	3	4	5
Empirical Formula	$C_{22}H_{17}Cu_2I_2N_6O_2$	$C_{22}H_{16}CuN_6O_2$	$C_{24}H_{20}Cu_2I_2N_7O_2$	$C_{11}H_9CuIN_3O$	$C_{63}H_{66}Cu_8I_8N_{15}O_7$
M	778.30	459.96	819.35	389.65	2668.83
Crystal system	Monoclinic	Orthorhombic	Monoclinic	Triclinic	Monoclinic
Space group	$P2_1/n$	*Pbca*	$P2_1/n$	*P*-1	*C2/c*
a/ Å	8.2450(10)	8.4693(6)	11.6390(9)	8.6202(6)	12.6943(3)
b/ Å	29.405(4)	14.3050(10)	15.3802(12)	9.0250(6)	32.7813(7)
c/ Å	10.8415(15)	15.7364(14)	14.9492(11)	9.2570(7)	24.8035(5)
α/°	—	—	—	69.480(4)	—
β/°	108.285(6)	—	99.3400(4)	69.496(4)	97.313(2)
γ/°	—	—	—	84.874(4)	—
V/Å^3	2495.7(6)	1906.5(3)	2640.6(3)	631.29(8)	10237.7(4)
Z	4	4	4	2	4
T/K	90(2)	90(2)	90(2)	90(2)	90(2)
μ/mm^{-1}	4.210	1.180	3.986	4.161	4.086
Reflections collected	43588	9112	32040	10220	28217
Unique reflections (R_{int})	4606(0.0414)	1739(0.0229)	4891(0.0233)	2340(0.0173)	9510(0.0501)
R_1 indices [$I>2\sigma(I)$]	0.0434	0.0313	0.0161	0.0154	0.0364
*wR*2 (all data)	0.1473	0.0787	0.0384	0.0630	0.0963

Table 1 Summary of crystallographic data

The Cu(II) ion adopted a distorted-octahedral coordination environment consisting of two chelating N_{py}, N_{ox} donor sets from two distinct $\mathbf{L^{23}}$ entities in the equatorial plane and two symmetry related axial I^- ions (Fig. 4). The axial I^- anion acted as a bridge between individual Cu(II) ions resulting in the formation of an infinite Cu(II) chain running along the [1 0 1] diagonal axis. The Cu–I bond lengths were 2.961(2) and 3.1488(15) Å. A search of the Cambridge Structural Database (CSD), version 5.33,[23, 24] for Cu(II)–I bonds showed 14 observations in 13 six-coordinate Cu(II) structures with an average Cu(II)–I distance of 3.23 Å. There were also 99 observations in 79 five-coordinate structures with an average Cu(II)–I distance of 2.83 Å. Combining these observations, the reported Cu(II)–I bond lengths vary from 2.56 to 3.51 Å. Given these findings, and the consequences of Jahn-Teller distortion, both Cu(II)–I distances could be considered to be genuine bonds.

An infinite 2D network was formed as a result of Cu(I) rhomboid dimers cross-linking each infinite Cu(II) chain (Fig. 5). These dimers were formed by Cu(I) adopting a pseudo-tetrahedral coordination environment (Fig. 5) consisting of two monodentate N_{py} donors from the three substituted pyridyl rings of two distinct $\mathbf{L^{23}}$ entities and two symmetry related I^- ions. Each $\mathbf{L^{23}}$ entity was bound to both a Cu(I) and Cu(II) ion. The Cu···Cu distance across the rhomboid dimer was found to be 2.559(2) Å.[25] The two $\mathbf{L^{23}}$ entities in the asymmetric unit, formed a bridged intramolecular oxime-oximato hydrogen bond.[26-30] The O–H···O distances were found to be 1.06(11) and 1.39(11) Å (corresponding to an O···O distance of 2.427(9) Å). The hydrogen was shared roughly equally between the two oxygen atoms, reflecting the strong oxime-oximato bridge.

Both $\mathbf{L^{23}}$ entities within the asymmetric unit acted as two-bladed chiral propellers, with the angles between the planes of the pyridyl rings corresponding to 52.02° and 77.14° (rings containing N1 and N4 respectively). Adjacent 2D networks stacked on top of one another giving a 3D network by virtue of a H-bonding interaction between the O2 atom and a nearby pyridyl ring H atom. The C–H···O distance was found to be 2.41 Å (corresponding to a C···O distance of 3.059(12) Å).

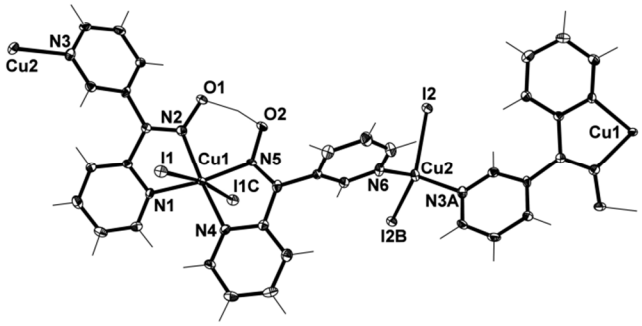

Fig. 4 View of the coordination environments of the Cu(I) and Cu(II) ions within **1** with crystallographic numbering. Thermal ellipsoids are drawn at 50% probability level. Selected bond lengths (Å) and angles (°): Cu(1)–N(1) 2.015(7), Cu(1)–N(2) 2.015(7), Cu(1)–N(4) 2.053(7), Cu(1)–N(5) 1.972(7), Cu(1)–I(1) 2.961(2), Cu(1)–I(1C) 3.1488(15), Cu(2)–N(3A) 2.065(7), Cu(2)–N(6) 2.087(8), Cu(2)–I(2) 2.599(2), Cu(2)–I(2B) 2.678(2), N(2)–O(1) 1.334(9), N(5)–O(2) 1.353(9); N(1)–Cu(1)–N(2) 79.3(3), N(1)–Cu(1)–N(4) 108.4(3), N(1)–Cu(1)–N(5) 172.1(3), N(1)–Cu(1)–I(1) 91.9(2), N(2)–Cu(1)–N(4) 166.9(3), N(2)–Cu(1)–N(5) 92.8(3), N(2)–Cu(1)–I(1) 101.6(2), N(4)–Cu(1)–N(5) 79.6(3), N(4)–Cu(1)–I(1) 88.9(2), N(5)–Cu(1)–I(1) 88.6(2), O(1)–N(2)–Cu(1) 123.1(5), O(2)–N(5)–Cu(1) 123.8(5), N(3)–Cu(2)–N(6) 99.2(3), N(3)–Cu(2)–I(2) 105.7(2), N(3)–Cu(2)–I(2) 112.9(2), N(6)–Cu(2)–I(2) 102.9(2), N(6)–Cu(2)–I(2) 111.3(2), Cu(2)–I(2)–Cu(2) 58.00(4), I(2)–Cu(2)–I(2) 122.00(4) (symmetry codes: A 1.5 – *x*, ½ + *y*, ½ – *z*; B 1 – *x*, – *y*, – *z*; C ½ – *x*, ½ + *y*, – ½ – *z*)

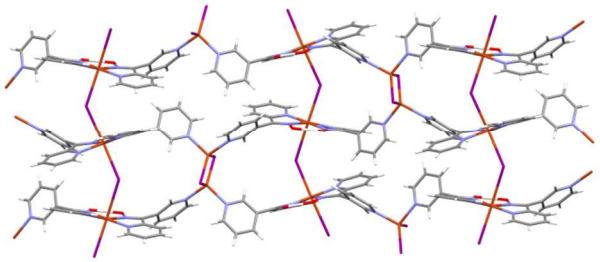

Fig. 5 View down the crystallographic *a* axis of the 2D network formed by **1**.

Complex **2** crystallised in the orthorhombic space group *Pbca* forming an infinite 2D network in the *ab* plane. The asymmetric unit contained half a Cu(II) cation and one deprotonated $\mathbf{L}^{23}$ ligand. No I^- anion was present despite the Cu(II) cation originating from Cu(I)I. Thus the Cu(I) ion was oxidised to Cu(II) and the resulting charge was balanced by deprotonation of the oxime unit of $\mathbf{L}^{23}$ which acted as a counterion. As this complex crystallized in a centrosymmetric space group, both enantiomeric forms of $\mathbf{L}^{23}$ were present in the 2D networks.

The Cu(II) ion sat on a centre of symmetry, adopting a Jahn-Teller distorted octahedral geometry. This consisted of two equatorial chelating (N_{py}, N_{ox}) donor sets from two $\mathbf{L}^{23}$ entities and two axial monodentate (N_{py}) donors from the three-substituted pyridyl ring of another two symmetry related $\mathbf{L}^{23}$ entities (Fig. 6). Thus, each Cu(II) ion was bound to four symmetry related $\mathbf{L}^{23}$ ligands. All nitrogen donors of $\mathbf{L}^{23}$ were involved in bonding to a Cu(II) ion allowing the ligand to act as a bridge between individual Cu(II) ions forming the 2D network (Fig. 7). This was reinforced by π-π stacking between the N1

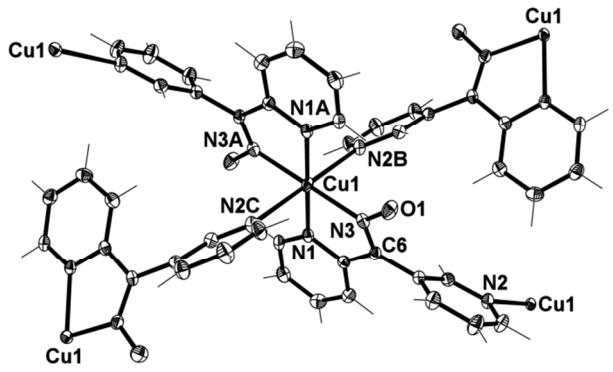

Fig. 6 View showing the coordination environment of the central Cu(II) ion in **2** with crystallographic numbering. Thermal ellipsoids are drawn at 50% probability level. Selected bond lengths (Å) and angles (°): Cu(1)–N(1) 2.038(2), Cu(1)–N(2) 2.428(2), Cu(1)–N(3) 2.030(2), C(6)–N(3) 1.310(3), N(3)–O(1) 1.294(3); N(1)–Cu(1)–N(3) 80.37(8), N(1)–Cu(1)–N(3A) 99.63(8), N(1)–Cu(1)–N(1A) 180.00(8), N(3)–Cu(1)–N(3A) 180.00(8), N(1)–Cu(1)–N(2D) 86.46(7), N(1)–Cu(1)–N(2E) 93.54(7), N(2D)–Cu(1)–N(3) 85.53(8), N(2E)–Cu(1)–N(3) 94.47(8), O(1)–N(3)–C(6) 120.1(2), O(1)–N(3)–Cu(1) 124.87(15), C(6)–N(3)–Cu(1) 114.41(16), C(6)–N(3)–O(1) 120.1(2) (symmetry codes: A – *x*, 1 – *y*, 1 – *z*; B – ½ + *x*, 1.5 – *y*, 1 – *z*; C ½ – *x*, – ½ + *y*, *z*).

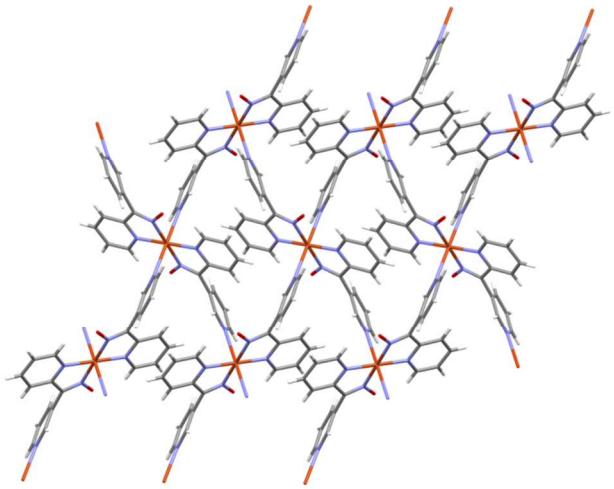

Fig. 7 View in the *ab* plane of the 2D network formed in **2**.

rings with a distance of 3.772(3) Å. The $\mathbf{L}^{23}$ ligand acted as a two-bladed chiral propeller with an angle of 58.45° between the planes of both pyridyl rings. No significant interactions were found to exist between individual 2D networks which ran parallel to each other.

$\{[Cu_2(L^{24})(L^{24}\text{-}H)I_2](CH_3CN)\}_\infty$, 3

Black X-ray quality crystals were grown from the slow diffusion of $\mathbf{L}^{24}$ in MeOH into a MeCN solution of CuI. Microanalysis of both the crystals and a bulk sample precipitated from 1:1 mix of MeCN and MeOH supported a 1:1 ligand-to-metal ratio. Notably, when the reaction was carried out in bulk the precipitate turned from initial red to dark brown.

IR analysis confirmed the presence of $\mathbf{L}^{24}$ within the bulk material. The shift in frequency of the C=N peak from 1604 cm^{-1} to 1653 cm^{-1} also implied that the N atom of the oxime functional group was bound to a Cu ion. The electronic spectrum of **3** showed a charge transfer band at 31 746 cm^{-1}. A second peak at 11 223 cm^{-1} was assigned to the *d-d* transition of the metal ion indicating the presence of Cu(II). Furthermore, the second peak was asymmetrical in nature with a small shoulder suggesting the Cu(II) ion was five coordinate possibly square pyramidal or Jahn-Teller distorted octahedral geometry.[22 31-33]

X-Ray structural analysis of **3** showed it crystallized in the monoclinic space group $P2_1/n$ forming a 1D mixed-valence infinite double chain along the *c* axis. The asymmetric unit contained two $\mathbf{L}^{24}$ entities of which one was deprotonated, one Cu(I) cation, one Cu(II) cation, two I^- anions and one MeCN solvent molecule. Both enantiomeric forms of $\mathbf{L}^{24}$ were found within the structure due to the centrosymmetric nature of the space group.

The Cu(II) ion adopted a square-based pyramidal geometry with two basal N_{py}, N_{ox} chelating donor sets, from two distinct $\mathbf{L}^{24}$ entities, and one axial I^- anion (Fig. 8). The τ_5 value for the Cu(II) ion was 0.30 supporting a distorted square pyramidal environment.[34] Bond angles around the Cu(II) ion ranged from 95.11(6) to 168.16(7)°. The Cu–N bond lengths ranged from 1.9580(18) to 2.0786(18) Å which fall within the range of 1.851 to 2.765 Å for similar five-coordinate systems as determined from a search of the CSD (version 5.34). [23, 24] The Cu–I bond length was elongated at 2.8577(9) Å, typical of square-based pyramidal complexes of Cu(II). This fell within the range 2.56 to

3.41 Å for similar systems. [23, 24] The Cu(I) adopted a tetrahedral coordination environment being bound to two I^- anions and two N_{py} atoms from the four-substituted pyridyl rings of two distinct ligands (Fig. 8). The τ_4 value for this Cu ion was found to be 0.29 indicating a distorted environment.[35] The bond angles around the Cu(I) ion ranged from 101.42(5) to 118.98(2)°. Both ligand entities within the asymmetric unit acted as a two-bladed chiral propellers, with the angles between the planes of the pyridyl rings corresponding to 68.97° and 67.58° (rings containing N2 and N5 respectively). The two $\mathbf{L^{24}}$ entities formed a bridged intramolecular oxime-oximato hydrogen bond.[26-30] The O–H···O distances were found to be 1.11(3) and 1.34(3) Å (corresponding to an O···O distance of 2.445(2) Å). In this case, the hydrogen is asymmetrically shared between the two oxygen atoms, again giving rise to a strong motif.

Each individual chain of the double chain contained only one enantiomeric form of the bridged motif with the other individual chain containing the other enantiomer.

Due to each ligand being bound to both Cu1 and Cu2 an infinite 1D chain of alternating Cu(I) and Cu(II) ions was formed along the *c* axis. The I1 anion acted as a μ_2 bridging ion between Cu(I) and Cu(II) ions of adjacent 1D chains forming an infinite double chain.

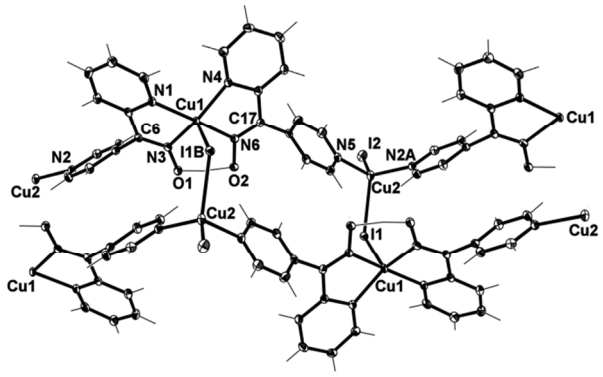

Fig. 8 View of the coordination environments of the Cu(I) and Cu(II) ions in **3** with crystallographic numbering. Thermal ellipsoids are drawn at 50% probability level. The CH_3CN solvent molecule has been omitted for clarity. Selected bond lengths (Å) and angles (°): Cu(1)–N(1) 2.0117(18), Cu(1)–N(3) 2.0264(18), Cu(1)–N(4) 2.0589(18), Cu(1)–N(6) 1.9580(18), Cu(1)–I(1) 2.8577(9), Cu(2)–N(2A) 2.0508(19), Cu(2)–N(5) 2.0786(18), Cu(2)–I(1B) 2.7220(11), Cu(2)–I(2) 2.5566(8), C(6)–N(3) 1.292(3), N(3)–O(1) 1.345(2), C(17)–N(6) 1.293(3), N(6)–O(2) 1.342(2); N(1)–Cu(1)–N(3) 79.91(7), N(1)–Cu(1)–N(4) 104.05(8), N(1)–Cu(1)–N(6) 168.16(7), N(3)–Cu(1)–N(4) 150.49(7), N(3)–Cu(1)–N(6) 91.10(8), N(4)–Cu(1)–N(6) 80.05(7), N(1)–Cu(1)–I(1) 97.54(5), N(3)–Cu(1)–I(1) 113.56(6), N(4)–Cu(1)–I(1) 95.11(6), N(6)–Cu(1)–I(1) 93.09(6), O(1)–N(3)–Cu(1) 125.12(13), O(2)–N(6)–Cu(1) 122.23(13), N(2A)–Cu(2)–N(5) 106.49(7), N(2A)–Cu(2)–I(1B) 102.66(5), N(5)–Cu(2)–I(1B) 101.42(5), N(2A)–Cu(2)–I(2) 116.23(5), N(5)–Cu(2)–I(2) 109.47(5), Cu(1)–I(1)–Cu(2) 123.51(2), I(1)–Cu(2)–I(2) 118.98(2) (symmetry codes: A *x*, *y*, 1 + *z*; B 1 – *x*, – *y*, – *z*).

The double chain network was further expanded into an infinite 2D network along the *bc* plane by virtue of a non-classical H-bonding interaction between the O2 atom and a nearby pyridyl ring H atom. The C–H···O distance was found to be 2.42 Å (corresponding to a C···O distance of 3.159(3) Å)

$[Cu(L^{33})I]_\infty$, 4

A 1:1 molar reaction between CuI and $\mathbf{L^{33}}$ in a 1:1 mix of MeCN and MeOH gave a cream precipitate in moderate-to-high yield. Microanalysis confirmed a 1:1 metal-to-ligand molar ratio. IR analysis confirmed the presence of $\mathbf{L^{33}}$ in the bulk material. Weak and poorly resolved peaks in the range 1638-1619 cm^{-1} were assigned to the C=N moiety and differed from the free ligand where a single peak was observed at 1615 cm^{-1}.[13] Yellow X-ray quality crystals were grown from the slow diffusion of $\mathbf{L^{33}}$ in MeOH into a MeCN solution of CuI.

X-Ray crystallographic analysis showed **4** crystallized in the triclinic space group *P*-1 forming an infinite 1D daisy chain (Fig. 9). The asymmetric unit consisted of one $\mathbf{L^{33}}$ entity, one Cu(I) cation and one I^- anion, with both enantiomeric forms of $\mathbf{L^{33}}$ present. The Cu(I) ion adopted a tetrahedral coordination environment consisting of two I^- anions and two three-substituted N_{py} atoms from two $\mathbf{L^{33}}$ entities. A rhomboid dimer was therefore formed, with a Cu···Cu distance of 2.5698(12) Å. The angles between the Cu(I) ion and its four donor atoms ranged from 105.84(8)° to 110.44(7)° indicating a distorted tetrahedral environment. The ligand itself acted as a two-bladed chiral propeller, with an angle of 71.05° between the planes of the pyridyl rings. This twist of the pyridyl rings relative to each other further supported the formation of the daisy chain.

The 1D daisy chain polymer formed from two $\mathbf{L^{33}}$ ligands bridging two Cu(I) ions of Cu_2I_2 connecting units propagated along the [1 0 1] diagonal axis (Fig. 9). Individual daisy chains stacked side by side though a non-standard H-bond between the oxime H atom and the I^- ion (Fig. 10) forming an infinite 2D sheet. The O–H···I distance was found to be 2.57 Å with a corresponding O···I distance of 3.458(3) Å. The 2D sheets were held together by a π-π bonding interaction from adjacent N1 pyridyl rings (centroid-centroid distance 3.649(3) Å).

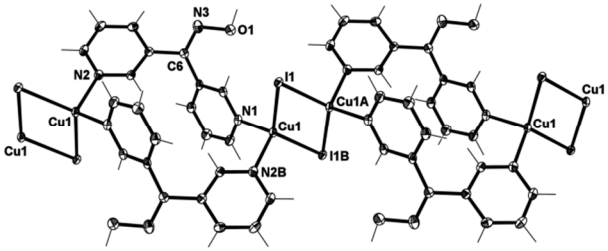

Fig. 9 View along [1 0 1] diagonal axis of **4** with crystallographic numbering. Thermal ellipsoids are drawn at 50% probability level. Selected bond lengths (Å) and angles (°): Cu(1)–N(1) 2.060(3), Cu(1)–N(2B) 2.060(3), Cu(1)–I(1) 2.6241(12), Cu(1)-(1B) 2.6642(11), C(6)–N(3) 1.288(4), N(3)–O(1) 1.392(4); N(1)–Cu(1)–I(1) 105.84(8), N(1)–Cu(1)–I(1B) 110.44(7), N(2B)–Cu(1)–I(1) 125.21(8), N(2B)–Cu(1)–I(1) 106.55(8), Cu(1)–I(1)–Cu(1A) 58.39(2), I(1)–Cu(1)–I(1B) 121.61(2), C(6)–N(3)–O(1) 112.0(3) (symmetry codes: A 1 – *x*, 1 – *y*, – *z*; B 1 – *x*, – *y*, 1 – *z*).

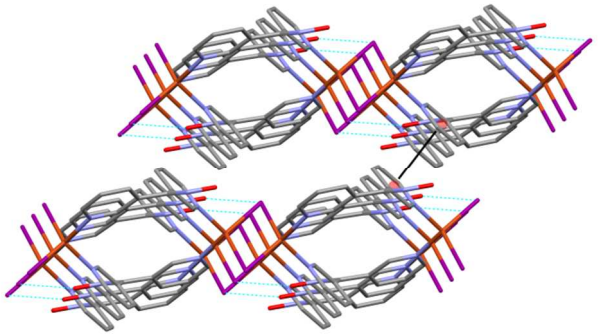

Fig. 10 View of the side by side stacking in **4** of individual 1D daisy chains that form 2D sheets by H-bonding (shown in green). The offset π-π stacking interaction that generates a 3D structure is shown as a solid black line.

$\{[Cu_8(L^{44})_5I_8](CH_3CN)_4(C_4H_{10}O)_2(H_2O)_2\}_\infty$, 5

X-ray analysis of **5** showed that it crystallised in the monoclinic space group *C2/c* as an infinite 2D network in the *ac* plane which was extended through hydrogen bonding into two 3D interpenetrated networks. The asymmetric unit consisted of four Cu(I) cations, four I^- anions, two and a half $\mathbf{L^{44}}$ entities, one diethyl ether molecule, two acetonitrile molecules and one water molecule. The acetonitrile and water molecules were very disordered, and could not be appropriately modelled. The electron density associated with the them was removed using the SQUEEZE procedure in PLATON.[36] This was supported by the large solvent spaces present in the structure.

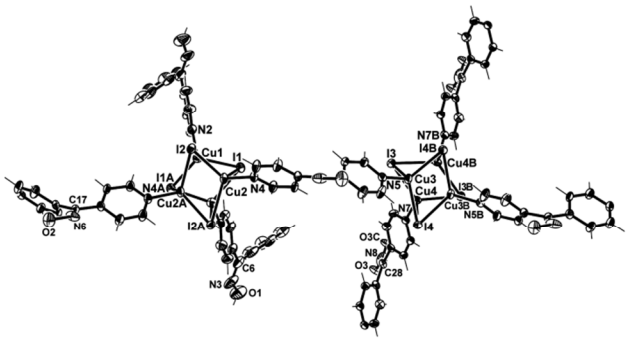

Fig. 11 View of the coordination environments of the Cu(I) ions in **5** with crystallographic numbering. Thermal ellipsoids are drawn at 50% probability level. Selected bond lengths (Å) and angles (°): Cu(1)–N(2) 2.016(5), Cu(1)–I(1) 2.6996(13), Cu(1)–I(1A) 2.7035(13) Cu(1)–I(2) 2.6556(13), Cu(2)–N(4) 2.008(4), Cu(2)–I(1) 2.7383(13), Cu(2)–I(2) 2.6427(12), Cu(2)–I(2A) 2.7729(13), Cu(3)–N(5) 2.033(4), Cu(3)–I(3) 2.7037(13), Cu(3)–I(4) 2.7236(13), Cu(3)–I(4A) 2.6524(13), Cu(4)–N(7) 2.014(4), Cu(4)–I(3) 2.6518(13), Cu(4)–I(3) 2.7483(13), Cu(4)–I(4) 2.7002(13), C(6)–N(3) 1.310(11), N(3)–O(1) 1.379(10), C(17)–N(6) 1.304(7), N(6)–O(2) 1.360(7), C(28)–N(8) 1.262(9), N(8)–O(3) 1.180(8); O(1)–N(3)–C(6) 110.2(6), O(2)–N(6)–C(17) 116.2(5), O(3)–N(8)–C(28) 127.1(4), range: I–Cu–I 103.73(3)–119.75(3), I–Cu–N 98.74(12)– 113.06(12), (symmetry codes: A 1 – *x*, *y*, 1.5 – *z*; B 2 – *x*, *y*, 2.5 – *z*; C 1 – *x*, *y*, 2.5 – *z*).

The N8 oxime sat on a special position, with the complete ligand generated by a two-fold axis along the N-C bond, and the O-H groups occupying two different sites. Each of the ligands acted as a two-bladed chiral propellers, with the angles between the planes of the pyridyl rings corresponding to 64.48 (N3), 64.44 (N6) and 64.18 (N8)

The Cu(I) ions were present in two crystallographically distinct Cu_4I_4 cubane tetramer clusters. These were linked by N_{py} ligands to form an infinite 2D network in the *ac* plane (Fig. 12). For one of the cubane tetramer clusters (Cu3, Cu4) all four ligands linked to other cubane tetramer clusters two of which were the same (Cu3, Cu4) and two of which were distinct (Cu1, Cu2). For the cluster (Cu1, Cu2) two of the ligands linked to other distinct clusters (Cu3, Cu4) while two did not link to clusters. These two ligands were involved in hydrogen bonding to an oxime unit on an adjacent network generating an infinite 3D structure with a O–H···N distance was found to be 1.97 Å with a corresponding O···N distance of 2.718(7) Å (fig. 13).

Overall, two 3D interpenetrated hydrogen bonded networks were generated, with no interactions between the two networks (Fig. 14).

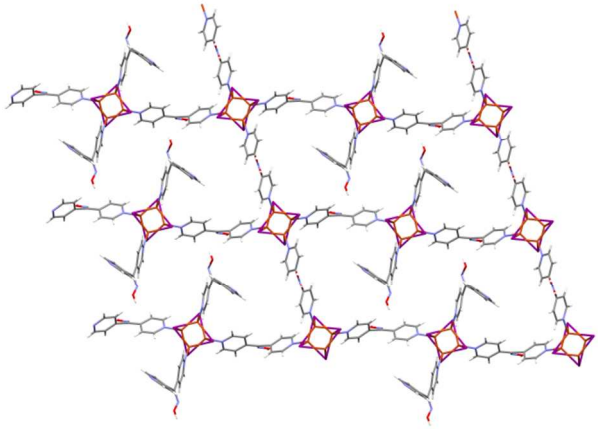

Fig. 12 View along *b* axis of **5**, showing infinite chains in the *ac* plane.

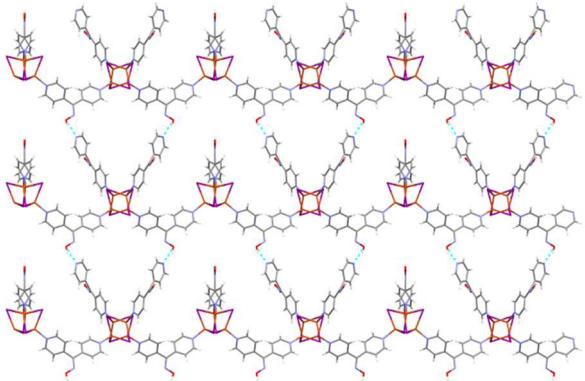

Fig. 13 View along *a* axis of **5** showing hydrogen bonds in green linking the structure into an infinite 3D network.

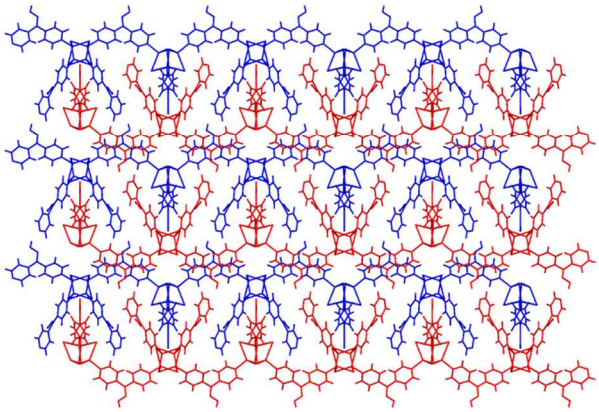

Fig. 14 View along *a* axis of **5** showing the 3D interlaced hydrogen bonded networks

Comparison

The five structures described herein provide elegant examples of the differing bonding arrangements of the ligands $\mathbf{L}^{23}$, $\mathbf{L}^{24}$, $\mathbf{L}^{33}$ and $\mathbf{L}^{44}$. Both $\mathbf{L}^{23}$ and $\mathbf{L}^{24}$ formed five-membered-chelate rings between the N_{ox} atom and two-substituted N_{py} atom upon coordination of a metal ion. In **1** and **3** these further extended into a pseudo tetradentate macrocycle through the presence of an oxime-oximato bridge between neighbouring ligands, providing a very stable coordination environment for Cu(II). By comparison, $\mathbf{L}^{33}$ and $\mathbf{L}^{44}$ cannot bind this way, and in **4** and **5** the {C=N–OH} moiety was consequently not involved in bonding interactions to Cu. This left it free to form H-bonding interactions, generating a larger polymer structure. The positioning of a N_{py} atom in the 3 or 4 position allowed the extension of the copper coordination into polymer structures for all complexes.

The role of the I^- anion cannot be ignored in the formation of the five structures reported. In **4** the 1D daisy chain was formed by virtue of I^- anions acting as a link between $\mathbf{L}^{33}{}_2Cu_2$ squares, giving rise to a typical rhomboid dimer motif. In complex **5** I^- anions formed Cu_4I_4 cubane tetramer clusters, allowing four ligands to bind to one centre. Both **1** and **3** were mixed-valence Cu(I)/Cu(II) polymers, formed as a result of partial oxidation of the Cu(I) ions from CuI. One of the ligand entities was deprotonated, acting as a charge balance along with the I^- anions. This resulted in the extension of the ligand into a pseudo tetradentate ligand through the presence of an oxime-oximato bridge in neighbouring ligands, which provided a very strong coordination motif for Cu(II).

These I^- anions also acted as vital linking anions in each of the structures. In **1** one of the two I^- anions formed part of a typical rhomboid dimer with the Cu(I) ion while the other acted as a bridging ion between symmetry related Cu(II) ions. The bonding arrangement of the I^- anions meant that a 2D network was formed. In **3** one of the two I^- anions present acted as a linking anion between the Cu(I) and Cu(II) ions, giving rise to the formation of a double chain. The second I^- anion was terminally bound assisting only in charge balance. This feature helped explain the 1D nature of the complex in comparison to the 2D nature of **1**. Finally, the structure in **2** lacked I^- anions as a consequence of the complete oxidation of Cu(I) to Cu(II) and the deprotonation of both ligand entities present. Thus, the ligands, which bridged between symmetry related Cu(II) ions, provided the necessary charge balance.

Conclusion

Five new coordination polymers were synthesised from CuI and a series of dipyridyl ketone oxime regio isomers ligands. Comparison of these polymers showed the importance of a pseudo tetradentate ligand formed via an oxime-oximato bridge on the formation of mixed valence Cu(I)/Cu(II) polymers. The key to forming such a coordination arrangement is through the extension of the five-membered chelate ring that can be formed between the 2-substituted pyridyl ring and the N atom of the oxime unit. We are currently investigating this strategy for the preparation of other mixed valence Cu(I)/Cu(II) coordination polymers.

Acknowledgment.

We acknowledge the Tertiary Education Commission New Zealand for the award of a Top Achiever Doctoral Scholarship (VJA) and thank the University of Otago Research Committee (VJA) and the University of Otago for financial support.

Notes and references

Department of Chemistry, Te Tari Hua-Ruanuku, University of Otago, P. O. Box 56, Dunedin,9054, New Zealand. Fax: (+64) 3–479–7906; Tel: (+64) 3–479–7918; E-mail: lhanton@chemistry.otago.ac.nz

† Electronic Supplementary Information (ESI) available: CIF files of the crystal structures. CCDC reference numbers CCDC 974173-974177

See DOI: 10.1039/b000000x/

1. R. Peng, M. Li and D. Li, *Coord. Chem. Rev.*, 2010, **254**, 1-18.
2. A. J. Blake, N. R. Brooks, N. R. Champness, L. R. Hanton, P. Hubberstey and M. Schroder, *Pure Appl. Chem.*, 1998, **70**, 2351-2357.
3. C. Housecroft and A. G. Sharpe, *Inorganic Chemistry* 4th edn., Pearson Education Ltd, Essex, 2012.
4. G. A. Bowmaker, N. C. Di, C. Pettinari, B. W. Skelton, N. Somers and A. H. White, *Dalton Trans*, 2011, **40**, 5102-5115.
5. P. Chaudhuri, M. Winter, U. Floerke and H.-J. Haupt, *Inorg. Chim. Acta*, 1995, **232**, 125-130.
6. E. S. Koumousi, C. P. Raptopoulou, S. P. Perlepes, A. Escuer and T. C. Stamatatos, *Polyhedron*, 2010, **29**, 204-211.
7. V. V. Ponomarova and K. V. Domasevitch, *Cryst. Eng.*, 2002, **5**, 137-145.
8. C. H. Liu and C. F. Liu, *J. Am. Chem. Soc.*, 1961, **83**, 4169-4172.
9. A. Chakravorty, *Coord. Chem. Rev.*, 1974, **13**, 1-46.
10. X. Qiu, L. Li and D. Li, *Acta Crystallogr., Sect. E: Struct. Rep. Online*, 2011, **67**, m1810-m1811.
11. B. Zhong, S. Li and G. Chen, *Acta Crystallogr., Sect. E: Struct. Rep. Online*, 2012, **68**, m874.
12. G. Wu and D. Wu, *Acta Crystallogr., Sect. E: Struct. Rep. Online*, 2008, **64**, m828, m828/821-m828/826.
13. V. J. Argyle, L. M. Woods, M. Roxburgh and L. R. Hanton, *CrystEngComm*, 2013, **15**, 120-134.
14. Z. Otwinowski and W. Minor, *Processing of X-Ray*

Diffraction Data Collected in Oscillation Mode, 1 edn., Academic Press: New York, 1997.

15. SAINT-V4, *Area Detector and Integration Software*, (1996) Siemens Analytical X-Ray Systems Inc., Madison, WI.
16. G. M. Sheldrick, *SADABS, Program for Adsorption Correction*, University of Göttingen, Göttingen, Germany, 1996.
17. A. Altomare, M. C. Burla, M. Camalli, G. L. Cascarano, C. Giacovazzo, A. Guagliardi, A. G. G. Moliterni, G. Polidori and R. Spagna, *Journal of Applied Crystallography*, 1999, **32**, 115.
18. G. M. Sheldrick, *Acta Crystallographica, Section A: Foundations of Crystallography*, 2008, **A64**, 112-122.
19. L. J. Farrugia, *Journal of Applied Crystallography*, 1999, **32**, 837.
20. C. F. Macrae, P. R. Edgington, P. McCabe, E. Pidcock, G. P. Shields, R. Taylor, M. Towler and J. van de Streek, *Journal of Applied Crystallography*, 2006, **39**, 453.
21. I. J. Bruno, J. C. Cole, P. R. Edgington, M. K. Kessler, C. F. Macrae, P. McCabe, J. Pearson and R. Taylor, *Acta Crystallogr., Sect. B*, 2002, **B58**, 389.
22. T. Murakami, S. Hatakeyama, S. Igarashi and Y. Yukawa, *Inorganica Chimica Acta*, 2000, **310**, 96.
23. F. H. Allen, *Acta Crystallogr., Sect. B*, 2002, **B58**, 380.
24. F. H. Allen, J. E. Davies, J. J. Galloy, O. Johnson, O. Kennard, C. F. Macrae, E. M. Mitchell, G. F. Mitchell, J. M. Smith and D. G. Watson, *Journal of Chemical Information and Computer Sciences*, 1991, **31**, 187.
25. X.-P. Zhou, D. Li, S.-L. Zheng, X. Zhang and T. Wu, *Inorg. Chem.*, 2006, **45**, 7119.
26. H. Kipton, J. Powell and J. M. Russell, *Aust. J. Chem.*, 1978, **31**, 2409-2416.
27. N. F. Curtis, O. P. Gladkikh, K. R. Morgan and S. L. Heath, *Acta Crystallogr., Sect. C: Cryst. Struct. Commun.*, 2004, **C60**, m256-m257.
28. V. Y. Kukushkin, T. Nishioka, D. Tudela, K. Isobe and I. Kinoshita, *Inorg. Chem.*, 1997, **36**, 6157-6165.
29. M. Watanabe, Y. Kashiwame, S. Kuwata and T. Ikariya, *Eur. J. Inorg. Chem.*, 2012, **2012**, 504-511.
30. V. Y. Kukushkin and A. J. L. Pombeiro, *Coord. Chem. Rev.*, 1999, **181**, 147-175.
31. B. J. Hathaway and D. E. Billing, *Coord. Chem. Rev.*, 1970, **5**, 143.
32. T. Murakami, T. Takei and Y. Ishikawa, *Polyhedron*, 1996, **16**, 89.
33. R. Kruszynski, B. Kuznik, T. J. Bartczak and D. Czakis-Sulikowska, *Journal of Coordination Chemistry*, 2005, **58**, 165.
34. A. W. Addison, T. N. Rao, J. Reedijk, R. J. Van and G. C. Verschoor, *J. Chem. Soc., Dalton Trans.*, 1984, 1349-1356.
35. L. Yang, D. R. Powell and R. P. Houser, *Dalton Transactions*, 2007, 955.
36. A. L. Spek, *J. Appl. Crystallogr.*, 2003, **36**, 7-13.

Table of Contents Synopsis

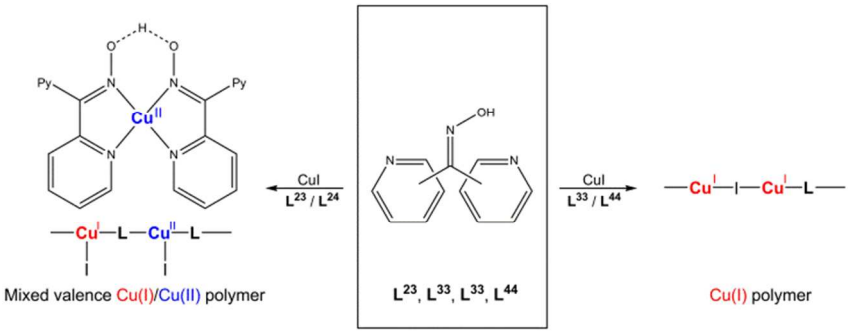

Coordination polymers formed from copper iodide and four isomeric dipyridyl ketone oxime ligands showed the importance the oxime-oximato bridge on the formation of mixed valence Cu(I)/Cu(II) polymers.